

RESEARCH ARTICLE

A quantitative experimental phantom study on MRI image uniformity

^{1,2}Doaa Felemban, ³Rinus G Verdonschot, ¹Yuri Iwamoto, ¹Yuka Uchiyama, ³Naoya Kakimoto, ^{1,4}Sven Kreiborg and ^{1,4}Shumei Murakami

¹Department of Oral and Maxillofacial Radiology, Osaka University Graduate School of Dentistry, Osaka, Japan; ²Department of Oral and Maxillofacial Radiology, College of Dentistry, Taibah University, Medina, Saudi Arabia; ³Department of Oral and Maxillofacial Radiology, Institute of Biomedical & Health Sciences, Hiroshima University, Hiroshima, Japan; ⁴3D Craniofacial Image Research Laboratory, School of Dentistry, Copenhagen University Hospital Rigshospitalet, University of Copenhagen, Copenhagen, Denmark

Objectives: Our goal was to assess MR image uniformity by investigating aspects influencing said uniformity via a method laid out by the National Electrical Manufacturers Association (NEMA).

Methods: Six metallic materials embedded in a glass phantom were scanned (*i.e.* Au, Ag, Al, Au–Ag–Pd alloy, Ti and Co–Cr alloy) as well as a reference image. Sequences included spin echo (SE) and gradient echo (GRE) scanned in three planes (*i.e.* axial, coronal, and sagittal). Moreover, three surface coil types (*i.e.* head and neck, Brain, and temporomandibular joint coils) and two image correction methods (*i.e.* surface coil intensity correction or SCIC, phased array uniformity enhancement or PURE) were employed to evaluate their effectiveness on image uniformity. Image uniformity was assessed using the National Electrical Manufacturers Association peak-deviation non-uniformity method.

Results: Results showed that temporomandibular joint coils elicited the least uniform image and brain coils outperformed head and neck coils when metallic materials were present. Additionally, when metallic materials were present, spin echo outperformed gradient echo especially for Co–Cr (particularly in the axial plane). Furthermore, both SCIC and PURE improved image uniformity compared to uncorrected images, and SCIC slightly surpassed PURE when metallic metals were present. Lastly, Co–Cr elicited the least uniform image while other metallic materials generally showed similar patterns (*i.e.* no significant deviation from images without metallic metals).

Conclusions: Overall, a quantitative understanding of the factors influencing MR image uniformity (*e.g.* coil type, imaging method, metal susceptibility, and *post-hoc* correction method) is advantageous to optimize image quality, assists clinical interpretation, and may result in improved medical and dental care.

Dentomaxillofacial Radiology (2018) 47, 20180077. doi: [10.1259/dmfr.20180077](https://doi.org/10.1259/dmfr.20180077)

Cite this article as: Felemban D, Verdonschot RG, Iwamoto Y, Uchiyama Y, Kakimoto N, Kreiborg S, et al. A quantitative experimental phantom study on MRI image uniformity. *Dentomaxillofac Radiol* 2018; 47: 20180077.

Keywords: magnetic resonance imaging; artefacts; dental radiography; metals

Introduction

MRI is a technique widely applied to investigate oral and maxillofacial disorders, such as temporomandibular

joint (TMJ) disorder, malignant tumours, inflammation, anatomical measuring purposes, and recently, as a diagnostic tool prior to dental implant insertion.^{1–5} MRI has several advantages over other methods (such as computed tomography, henceforth CT); *e.g.* it elicits high soft tissue contrast, does not expose patients

Correspondence to: Dr Rinus G Verdonschot, E-mail: rinusverdonschot@gmail.com

Received 23 February 2018; revised 27 March 2018; accepted 11 April 2018

to ionizing radiation, and allows for the selection of optional tomographic planes.⁶⁻⁸ However, compared to CT the scanning time is considerably longer (thereby prolonging patient exam times) and importantly, the *spatial resolution* of MRI is usually lower than CT.⁹

Nowadays, to enhance the relatively lower spatial resolution, MRI is performed using arrays of (small) surface coils placed near the body.¹⁰ The advantage of using surface coils (over whole body/volume coils) is that they provide higher radiofrequency sensitivity over small, specifically selected, portions of the body. Consequently, they obtain a much higher signal-to-noise ratio within the target area than would be possible from larger, usually more distant, coils (*i.e.* whole body/volume coils).¹⁰ The size and configuration of the surface coil (*i.e.* consisting of one or more coils forming a specific configuration) is often optimized for a specific region of interest. For example, in the oral and maxillofacial region (OMR), the TMJ and the head and neck (HN) coil are often used to improve the spatial resolution at these respective locations.¹¹ Many surface coils (including the HN and brain coils) are of the phased array coil type. These are a type of surface coil containing several surface coil elements or channels (each having its own receiver) allowing for parallel imaging, thereby covering a larger area and speeding up scanning time, as well as providing enhanced signal-to-noise ratio.¹⁰ However, when using surface coils (particularly phased array coils), overall signal uniformity may become severely impaired.^{10,12}

The nature of the surface coil configuration for any clinical investigation may have a significant impact on the diagnostic outcome.¹³ For example, if the target of investigation is a structure in the *centre* of the OMR (such as the tongue), using an inappropriate phased array coil might lead to a misdiagnosis of non-targeted tissues due to the influence of the surface coil on the overall uniformity of the MR image. This occurs as the penetration depth of the radio frequency signal depends on the coil's specifications and may lead to the situation that signals emanating from the body that are close to the coil are heightened while those originating more deeply in the body are reduced (as the coil receives less signal outside its target area).¹³ Therefore, when investigating the tongue using an inappropriate surface coil; signals from the parotid glands (located closer to the surface on either side of the mouth) might become very bright due to their proximity to the coil. This might lead a physician to inaccurately diagnose, for example, a lesion in the parotid gland (where, in fact, none exists) due to inappropriate coil selection.

The notion that the MR image uniformity indeed constitutes an important factor is illustrated by the fact that MRI scanner manufacturers have devised several methods to improve the non-uniformity of the image.¹⁴ These methods are routinely used when imaging the body (although some of these measures are in specific cases not recommended, for instance when performing

fMRI). Image correction methods can be classified in two groups, (1) applying filters after scanning (*post-hoc* filters) and (2) pre-scan calibration mapping. The *post-hoc* filters are also called *surface coil intensity correction* (SCIC) filters and typically apply a low-pass filter after MR scanning is completed.¹⁵ Consequently, rough image contrasts can be derived from this filter and brighter areas will be darkened and darker areas will be brightened using contrast mapping to achieve more optimal image uniformity. The second method (*e.g.* called "phased array uniformity enhancement" or PURE for GE scanners, or "pre-scan normalize" for Siemens scanners) performs specific initial sensitivity calibration scans before the actual imaging starts that will be used to optimize the actual diagnostic MR images. Notably, it has been speculated that methods like PURE or "pre-scan normalize" might not be optimal when metallic materials are present in the to-be-scanned area as these materials may hamper coil calibration thereby even worsening the resulting images in some cases.¹³

To avoid mishaps in clinical diagnosis as a result from non-optimal images, it is sensible to investigate the effects that different types of surface coils elicit on the uniformity of the magnetic field in combination with the presence of metallic materials, but, as far as we know, little attention has been focused on this topic. Yet, one recent study focused on the effects dental metals have on MR image quality.¹⁶ This study quantitatively standardized artefact volume and configurations (according to ASTM guidelines) and found significant differences between material composition, scanning sequences and scanning plane.^{16,17} However, they did not consider any effects on field uniformity depending on surface coil configuration as well as the effect of available methods for correcting the inhomogeneity. Therefore, the main aims of the current study were fourfold: (1) assessment of MR image uniformity depending on three distinctive, often used, surface coil types, (2) assessment of MR image uniformity depending on the tomographic plane, (3) assessment of MR image uniformity depending on the imaging sequence, and (4) assessment of the effectiveness of the coil intensity correction techniques (*i.e.* SCIC and PURE). All these four aims are important specifically in relation to whether (frequently encountered) metallic materials were present in the to-be-scanned area or not.

We investigate this matter further by means of the non-uniformity index (NUI) which has been advanced by the National Electrical Manufacturers Association (NEMA) as a suitable standardized measure to investigate magnetic field uniformity.¹⁸ This study, therefore, provides a comprehensive quantitative assessment of various important variables (*i.e.* scanning sequence, imaging plane, coil correction method, and presence of metallic material), which can influence MR image uniformity. The information contained in this article can, therefore, meaningfully inform clinicians and avoid

Table 1 Composition of the used materials and their magnetic susceptibility

Pure metal	Element symbol	Magnetic susceptibility (110^{-8} $\text{cm}^3 \text{mol}^{-1}$)
Gold	Au	-28.0
Silver	Ag	-19.5
Aluminium	Al	16.5
Titanium	Ti	151.0
Chromium	Cr	167.0
Cobalt	Co	ferro.
Copper	Cu	-5.5
Palladium	Pd	540.0
Molybdenum	Mb	72.0
Alloy composition		
Au–Ag–Pd alloy	Au (12%), Ag (51%), Pd (20%), Cu (15%)	
Co–Cr alloy	Co (63%), Cr (30%), Mo (5%)	

Ferro, ferromagnetic.

misinterpretation due to inappropriate coil, sequence or correction method selection.

Methods and materials

Samples and phantom

To evaluate the effect of metallic materials on MR image uniformity, six commonly used dental metallic materials were employed, specifically: gold (Au), silver (Ag), aluminium (Al), gold–silver–palladium (Au–Ag–Pd) alloy, titanium (Ti) and cobalt–chromium (Co–Cr) alloy. See Table 1 for the characteristics of the sample materials used. In line with ASTM standards each sample involved a 1 cm³ cube which was suspended by a nylon rod inside a cubic phantom (20 cm³) made of glass (SiO₂) and filled with 5% copper sulphate (CuSO₄) solution.^{16,17} All cubic metals were made in Kojundo Chemical Laboratory Co., Ltd (Saitama, Japan). For

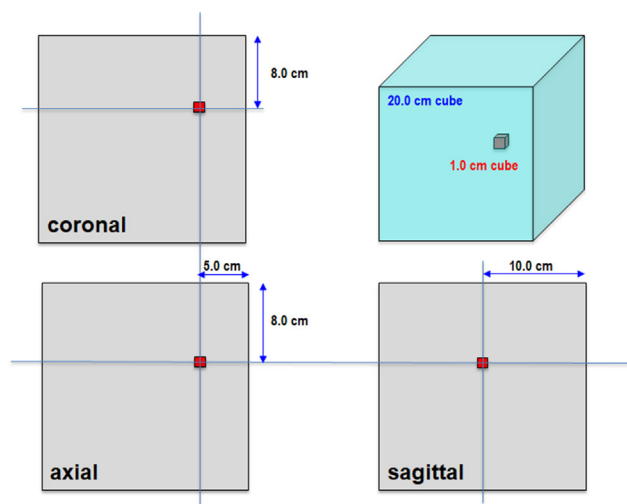


Figure 1 Position of the sample inside the phantom.

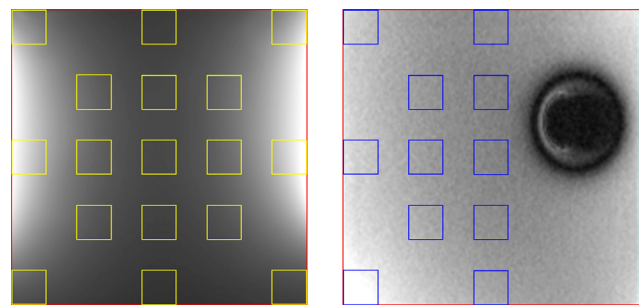


Figure 2 Left: standardized 17-point measurement (when no metallic material is present) method based on NEMA.¹⁸ Right: standardized 11-point (when metallic material, in this case Co–Cr, was present) measurement method based on NEMA.¹⁸ NEMA, National Electrical Manufacturers Association.

anatomical accuracy, the position of the sample in the phantom (*i.e.* $x = 5$ cm, $y = 8$ cm, $z = 10$ cm; Figure 1) roughly mimicked a position in the molar area in a typical human subject (Figure 1).

MRI

The phantom was subsequently scanned five times (average + standard error is reported) using the following coils (1) HN coil; 8-channel neurovascular MRI coil by GE (Milwaukee, WI) (GE: 800121), (2) brain coil; 8-channel high-resolution coil by GE (GE: 2317112-2), and (3) TMJ coil; 2-channel phased array coil by GE (GE: 46-307144 G6) on the cradle of a 1.5 T superconducting magnet scanner (GE Signa® HDxt 1.5 T MR; General Electric, Milwaukee, WI). Imaging parameters were selected according to ASTM-F2119 standards.¹⁷ The number of slices was 26, each slice thickness was 5 mm, and the interval between slices was 1 mm. For each examination, the phantom was scanned in the axial (vertical to the main magnetic field), coronal (parallel to floor), and sagittal planes (vertical to axial and coronal planes), using spin echo (SE) and gradient echo (GRE) sequences, with the following parameters: field of view: 20 cm by 20 cm, matrix size: 256 by 256 (*i.e.* pixel size; 0.8 mm), time to repetition: 500 ms, time to echo: 10 ms, number of excitations: 1, flip angle in GRE: 30° (according to ASTM-F2119 standards).¹⁷

Coil correction method

We evaluated the images under three different conditions, (1) no coil correction, henceforth: uncorrected, (2) using the *post-hoc* SCIC method (GE electronics) and (3) using the pre-scan PURE method (GE electronics).

Uniformity evaluation

To evaluate the uniformity of the images, we measured the signal intensity (SI) at 17 sample points according to the standardized sample method laid out by NEMA (Figure 2, left side) which allows for successive calculation of a NUI for each image (see Equation 1).¹⁸ The 17-point measurement was used when no metallic material was present in the phantom, when a metallic

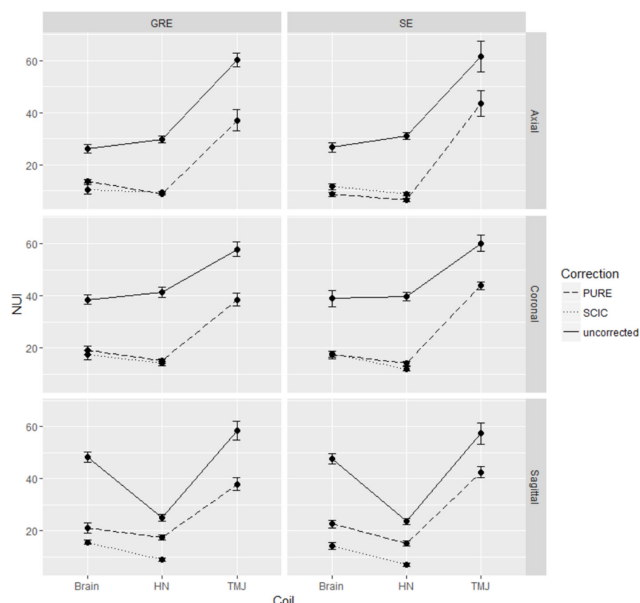


Figure 3 NUIs (in %; lower means more uniform) based on 17 sampling points without metallic materials by coil type and scanning plane. Legend indicates the specific correction method (uncorrected, PURE or SCIC). Note: there is no SCIC correction for the TMJ coil. NUI, non-uniformity index; PURE, phased array uniformity enhancement; SCIC, surfacecoil intensity correction; TMJ, temporomandibular joint.

material was present we used an adjusted 11 sample point measurement (Figure 2, right side) to avoid influencing the uniformity assessment due to the strong presence of the artefact. For NUI comparisons for two groups, such as between SE and GRE sequences, we employed a Mann–Whitney U test with the null hypothesis that there were no significant differences between the groups (significance levels set at $p < 0.01$). Similarly, for the NUIs amongst more than two groups we used the Kruskal–Wallis test similarly assuming no significant difference between the groups to be the null hypothesis (significance: $p < 0.01$). Furthermore, we used Wilcoxon signed-ranks tests to evaluate the multiple comparisons amongst conditions (significance: $p < 0.01$)

$$NUI = \frac{SI_{max} - SI_{min}}{SI_{max} + SI_{min}} \times 100 \quad (1)$$

Equation used in deriving the NUI based on SI, whereby 100% is extremely non-uniform and 0% is extremely uniform.¹⁸

Results

Results without metallic materials

First, we evaluated the results without the presence of metallic materials. As can be seen in Figure 3 below, the patterns were similar amongst the two scanning sequences (SE vs GRE) and were not significantly different ($W = 291.5$, $p = 0.95$) from each other. There

was an effect of coil type, $\chi^2(2) = 22.6$, $p < 0.001$; pairwise comparisons showed that the TMJ coil elicited the least uniformity across the board (*i.e.* significantly different from the Brain and HN coils, all p 's < 0.001), however, HN coils showed a similar pattern to Brain coils ($p = 0.16$). A Kruskal–Wallis rank sum test indicated that the scanning plane showed similar uniformity patterns across conditions, $\chi^2(2) = 2.1$, $p = 0.35$. There was a significant effect of correction method, $\chi^2(2) = 26.1$, $p < 0.001$. Pairwise comparisons showed that both SCIC ($p < 0.001$) and PURE ($p < 0.001$) elicited greater uniformity compared to uncorrected images, although, according to our conservative $p < 0.01$ threshold, PURE and SCIC themselves did not significantly differ from each other ($p = 0.02$).

Results with metallic materials

As can be seen in Figure 4, contrasting the earlier results without metallic materials, scanning sequences (SE, GRE) did show significant differences from each other ($W = 12,580$, $p < 0.01$) with SE being less influenced by metallic artefacts and eliciting more uniformity. Judging from Figure 4, this pattern might originate from the diverging effects of the two sequences in the Co–Cr and Ti metals. There was an effect of coil type, $\chi^2(2) = 95.7$, $p < 0.001$; pairwise comparisons showed that TMJ coils elicited the least uniformity across the board (being significantly different from brain and HN coils, all p 's < 0.001). Additionally, HN coils on average also showed slightly better uniformity over brain coils ($p < 0.01$) which, judging from Figure 4, might to some extent depend on the correction method used (*i.e.* SCIC vs PURE). Consequently, we found that HN coils were least susceptible to metallic artefacts, closely followed by brain coils and TMJ coils were most susceptible to metallic artefacts. A Kruskal–Wallis rank sum test indicated that the scanning plane showed similar uniformity patterns across conditions, $\chi^2(2) = 3.4$, $p = 0.19$. There was a significant effect of the correction method, $\chi^2(2) = 108.6$, $p < 0.001$. Pairwise comparisons showed that both SCIC ($p < 0.001$) and PURE ($p < 0.001$) on the whole elicited greater uniformity compared to uncorrected images; although on two occasions (*i.e.* Figure 4 top row Au–Ag–Pd and Co–Cr) uncorrected was close to PURE (which may represent a ceiling effect). Overall (Figure 4), SCIC elicited greater uniformity compared to PURE ($p < 0.001$) although for the TMJ coil no SCIC measurement was possible (*i.e.* limiting this outcome to the brain and HN coils). There was an effect of which metallic metal was present in the phantom, $\chi^2(5) = 40.5$, $p < 0.001$. Pairwise comparisons showed that Co–Cr differed from all the other metals (all p 's < 0.001). Particularly, Co–Cr elicited the *least* uniformity amongst all tested materials, which was especially evident in the GRE sequence and showed similar patterns for coil type as well as correction method.¹⁹ The other metals (*i.e.* Ag/Al/Au/Au–Ag–Pd/Ti) did not elicit statistically different effects on image uniformity (*i.e.* lowest $p = 0.39$).

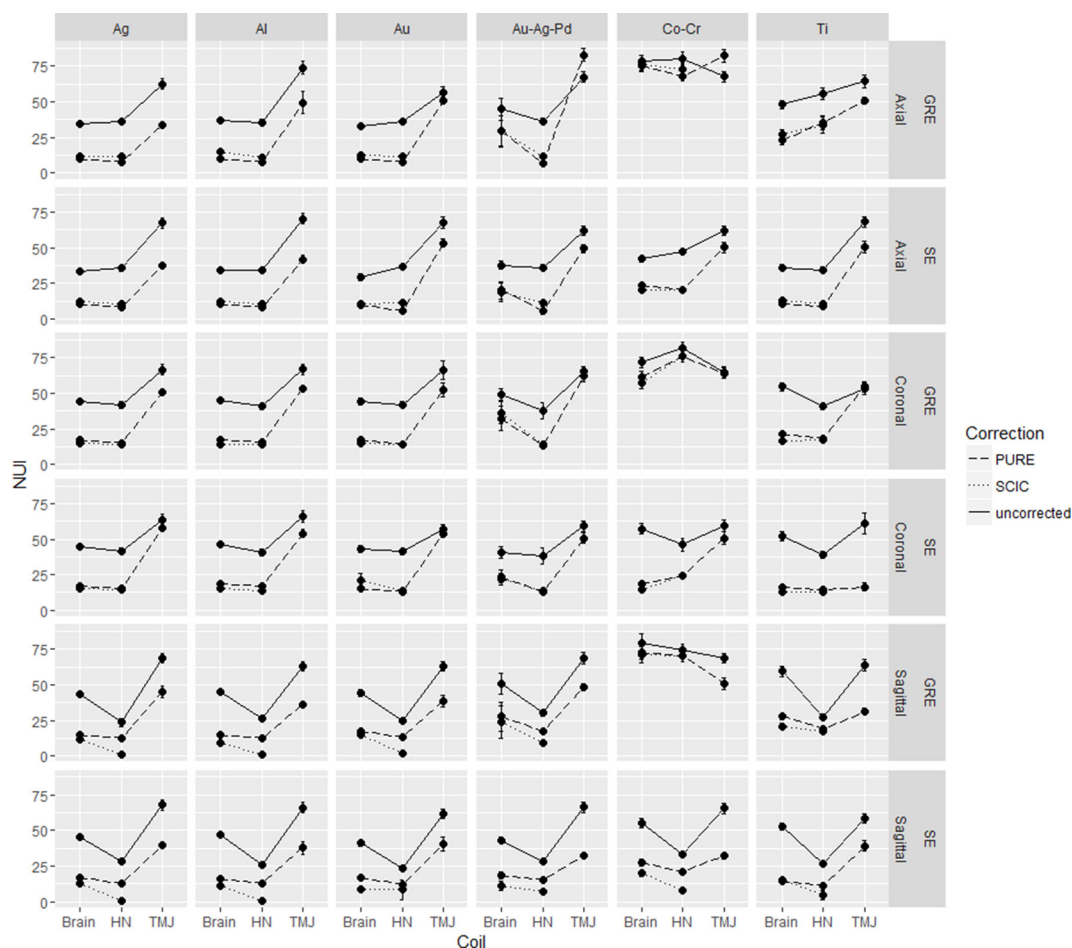


Figure 4 NUIs (in %; lower means more uniform) based on 11 sampling points without metallic materials by material, coil type and scanning plane. Legend indicates the specific correction method (uncorrected, PURE or SCIC). Note: there is no SCIC correction for the TMJ coil. NUI, non-uniformity index; PURE, phased array uniformity enhancement; SCIC, surfacecoil intensity correction; TMJ, temporo mandibular joint.

Discussion

This study investigated the effects of three surface coils (HN, brain, TMJ) on image uniformity in three orthogonal scanning planes using two MR sequences (SE, GRE) in combination with a phantom which contained six various, widely used in dental field, metallic materials (Au, Ag, Al, Au–Ag–Pd, Ti, and Co–Cr). Additionally, we investigated the effects of two frequently used image uniformity correction measures (*i.e.* SCIC, PURE) on the homogeneity of the MR images.

We found that when there was no metallic material present in the phantom the exact scanning sequence (SE, GRE) did not affect image uniformity in any combination of plane, coil type or image correction method, although SE elicited more uniformity when metallic materials (especially, Ti and Co–Cr) were present. When investigating the effect of coil type, we found that the TMJ coil always elicited the lowest uniformity whether or not metallic metals were present. When no metals were present, both HN and brain coils

did not differ greatly, although the HN coil elicited a larger uniformity when metals were present compared to the brain coil (which was most pronounced when applying SCIC). The scanning plane itself did not have any effect on uniformity measures in any condition. The two image correction methods (PURE, SCIC) typically showed improved uniformity compared to uncorrected images, however, SCIC generally outperformed PURE when metallic metals were present. Lastly, Co–Cr typically elicited the least uniform image quality while all the other metallic materials generally showed similar patterns across the board.

NUI assessment method

It is worth mentioning why this method to calculate image uniformity was chosen as there are several other calculation methods available. For example, the American College of Radiology provides another precise calculation method.¹⁹ Also, the NEMA, besides the 17-point calculation method we employed (using peak-deviation non-uniformity), also offers ways to produce greyscale

uniformity maps and/or determining the absolute averaged deviation uniformity. Although each method has its specific advantages and disadvantages, we opted to use the peak deviation non-uniformity method (using 17 or 11 points) as the NEMA guidelines specify this to be *especially suitable* to assess image intensity uniformity when using surface coils.¹⁸

Surface coil selection

Another point worth discussing concerns the selection of specific MR surface coils. Looking at our results, we found that HN coils show slightly better uniformity compared to brain coils (when metals are present) and this is especially noticeable when SCIC is applied within the sagittal plane (but not when Co–Cr is present). In absolute terms, image uniformity is still relatively high, even for the brain coil, which is significant for axial and sagittal slices which are often used in brain imaging.²⁰ Additionally, the HN coil aims for a wide range coverage from top of the head to upper chest area. Consequently, due to its relatively high uniformity it seems very suitable to get a uniform image in three planes for this larger region. Lastly, both HN and brain coils show better uniformity compared to TMJ coils irrespective of condition. However, since the TMJ coil is not used to image the whole HN region, its low uniformity should not become a significant problem for clinical investigation when focusing on the TMJ.²¹ However, in some special diagnostic cases, when administration of contrast media and examination with HN coil is required, the TMJ coil alone can achieve good results.²¹

Scanning sequence selection

We employed two often used sequences in this study (*i.e.* SE and GRE). One disadvantage of GRE (compared to SE) is that it is more susceptible to the inhomogeneity of the magnetic field especially when metallic materials are present (especially those with high magnetic susceptibility, [Table 1](#)).²² In this study, when there was no metallic material in the phantom, NUIs using GRE were not different from those using SE. However, when a metal with larger magnetic susceptibility was set (*e.g.* Co–Cr), NUIs using GRE were significantly higher than those using SE. Therefore, for clinical diagnostic imaging, our data indicate that it is necessary to assess which metal is set in the body, determine its magnetic susceptibility, and then select the appropriate sequence to obtain minimal MR image uniformity disturbance.

Image correction method

As stated in the “Introduction”, when applying a surface coil, overall image uniformity becomes affected. This is evidenced by the existence of various methods (*e.g.* SCIC, PURE) provided by MR scanner manufacturers to alleviate this problem. Our study shows that both SCIC and PURE significantly improved image uniformity; although SCIC generally outperformed PURE when metallic metals were present in the phantom.

One word of caution concerning these results is that SCIC uses low-pass filters to correct image uniformity, therefore, occasionally, truly significant high intensity areas may also be filtered out as a result. For example, on T_2 weighted images, most malignant tumours elicit strong intensity areas, so the possibility exists that true lesions could go unnoticed through the filtering process, thereby resulting in a non-optimal diagnosis. Additionally, an MRI image uniformity analysis of the liver showed an improvement in the image uniformity by using SCIC and PURE. However, they depended on a visual, subjective evaluation in the assessment of uniformity.²³ Yet, another phantom study,²⁴ showed that SCIC attained high in-plan uniformity values; while, on the other hand, PURE portrayed better cross slice uniformity. However, this study employed the ACR guidelines across different slices, and without standardized metal cube utilization.

Metallic materials

In daily practice, a patient’s body (*e.g.* especially in the OMR) may contain metals and/or alloys. Therefore, it is necessary to assess the effects of commonly used metallic materials on image uniformity. In this study, gold (Au) and silver (Ag) were examined as noble metals (and Au–Ag–Pd alloy as a noble metal alloy). Titanium (and occasionally aluminium) base metals were also examined as they are often used in medical and dental procedures (*e.g.* pins, screws and implants).²⁵ Lastly, cobalt (Co) chromium (Cr) alloy was also examined as it is often used in medical and dental prosthetics (such as artificial joints and dental implants).²⁶ When any metallic material is set in a strong magnetic field, the material will be magnetized. The exact degree of the magnetization is called the *magnetic susceptibility* ([Table 1](#) for an overview). As previous research indicated, large metallic artefacts appear on MRI images resulting from the presence of metallic materials the question is whether they would also impair overall image uniformity.²⁷ However, when we combined the data when no metal was present (*i.e.* 17-point method) with the data when metallic metals were present (11-point method) pairwise comparisons using the Wilcoxon ranked sum test showed that this was the case only for Co–Cr ($p < 0.001$) but not for any of the other materials (all p ’s > 0.43) even when the TMJ coil was not included in the analysis. This indicates that local non-uniformity originating from the metals position in the phantom (*i.e.* at the excluded 6 points), except for Co–Cr, did not significantly affect the overall uniformity in our phantom study. What is obvious, although, is that the GRE sequence should be avoided when Co–Cr is present.

Study limitations

This study used a 20 cm³ cubic phantom made of glass (SiO₂) filled with 5% copper sulphate (CuSO₄) solution following ASTM recommendations (*i.e.* T_1/T_2 relaxation times for CuSO₄ are well known, and glass does

not produce any artefacts or distortions).³ The phantom size approximated a human head and the size (*i.e.* 20 cm³) and position of the metallic material (which was 1 cm³ in size) was comparable to a commonly encountered clinical situation (*e.g.* a tooth crown in the molar area). However, a phantom based approach does not correct for any patient-induced inhomogeneity, which is a clear limitation of this study. However, as it is important to first establish an unbiased measure of image uniformity this would be difficult to achieve otherwise. Nevertheless, patient specific situations may evoke different patterns compared to this study, *e.g.* more fillings (of varying types) are usually present in patients, and although the current results therefore are informative, they only serve as a guideline. Future research will be needed, involving a larger mixture of different kinds of metals, to more accurately reflect clinical situations.

Implications for the dentistry field

Our results showed that image uniformity was always degraded (although the extent varied) for areas which were near the coils. Therefore, paying attention to non-uniformity is especially important when performing diagnoses at lateral sites (such as the parotid gland and the TMJ). For example, when inflammatory diseases are investigated (*e.g.* mumps, sialoadenitis, Sjögren syndrome) around the parotid gland, the application of SCIC or PURE is recommended to improve image uniformity (although for other conditions, such as: pleomorphic adenomas or Warthin's tumour; it is usually more important to focus on the existence and configuration of the condition without a specific need for image correction). Similarly, for quantitative diagnoses at the TMJ (*i.e.* dislocation and deformity of the articular disk) image correction is not a major factor, however, when diagnosing joint effusion or change in bone structure at the TMJ condylar head, SCIC or PURE in combination with adequate sequence selection is recommended as this may correct for any non-uniformity (*i.e.* as SI is used as

an indicator to make an accurate diagnosis). Similarly, our study shows that non-uniformity was particularly high for areas which were close to metallic materials for which the magnetic susceptibility is high (*e.g.* Co–Cr). Although we can reasonably neglect this non-uniformity when configuration diagnosis is performed in the OMR (*i.e.* tumour existence, tumour extension), when diagnosing inflammatory conditions (*e.g.* osteomyelitis or mucositis), however, the appropriate sequence and coil selection may matter a great deal as SI plays an important part as a diagnostic indicator.

Conclusion

This study assessed MR image uniformity by investigating several aspects expected to influence image uniformity during MR scanning (*i.e.* coil type, image correction method, scanning plane and sequence, and metallic material). We found that the TMJ coil typically elicited the least uniform image compared to brain and HN coils. When metallic materials were present, the HN coil slightly outperformed the brain coil. Additionally, when metallic materials were set, the SE sequence slightly outdid GRE especially for Co–Cr (and perhaps also Ti) most noticeably in the axial plane. Next, both SCIC and PURE improved image uniformity compared to uncorrected images, and SCIC slightly outperformed PURE when metallic metals were present. Lastly, Co–Cr elicited the least uniform image while all the other metallic materials generally showed similar patterns across the board (which did not deviate significantly from images without metallic metals present).

We conclude that a quantitative understanding of the various factors influencing image uniformity represent an important addition in optimizing image quality and clinical interpretation. This may potentially lead to the avoidance of image misinterpretation (due to for instance coil flaring), and consequently may advance overall medical and dental care.

References

1. Hegab AF, Youssef AH, Hameed H, Karam KS. MRI-based determination of occlusal splint thickness for temporomandibular joint disk derangement: a randomized controlled clinical trial. *Oral Surg Oral Med Oral Pathol Oral Radiol* 2018; **125**: 74–87. doi: <https://doi.org/10.1016/j.oooo.2017.09.017>
2. Alsaffar HA, Goldstein DP, King EV, de Almeida JR, Brown DH, Gilbert RW, et al. Correlation between clinical and MRI assessment of depth of invasion in oral tongue squamous cell carcinoma. *J Otolaryngol Head Neck Surg* 2016; **45**: 61–5. doi: <https://doi.org/10.1186/s40463-016-0172-0>
3. Xu Z, Koo A, Shah A. The utility of MRI for the diagnosis of osteomyelitis in the pressure ulcer patient. *J Plast Reconstr Aesthet Surg* 2017; **70**: 289–91. doi: <https://doi.org/10.1016/j.bjps.2016.11.009>
4. Loures FB, Carrara RJ, Góes RFA, Albuquerque R, Barretto JM, Kinder A, et al. Anthropometric study of the knee in patients with osteoarthritis: intraoperative measurement versus magnetic resonance imaging. *Radiol Bras* 2017; **50**: 170–5. doi: <https://doi.org/10.1590/0100-3984.2016.0007>
5. Imamura H, Sato H, Matsuura T, Ishikawa M, Zeze R. A comparative study of computed tomography and magnetic resonance imaging for the detection of mandibular canals and cross-sectional areas in diagnosis prior to dental implant treatment. *Clin Implant Dent Relat Res* 2004; **6**: 75–81. doi: <https://doi.org/10.1111/j.1708-8208.2004.tb00029.x>
6. Chun CW, Jung JY, Baik JS, Jee WH, Kim SK, Shin SH. Detection of soft-tissue abscess: comparison of diffusion-weighted imaging to contrast-enhanced MRI. *J Magn Reson Imaging* 2018; **47**: 60–8. doi: <https://doi.org/10.1002/jmri.25743>
7. Coran A, Ortolan P, Attar S, Alberioli E, Perissinotto E, Tosi AL, et al. Magnetic resonance imaging assessment of lipomatous soft-tissue tumors. *In Vivo* 2017; **31**: 387–95. doi: <https://doi.org/10.21873/invivo.11071>

8. Musgrave MT, Westesson PL, Tallents RH, Manzione JV, Katzberg RW. Improved magnetic resonance imaging of the temporomandibular joint by oblique scanning planes. *Oral Surg Oral Med Oral Pathol* 1991; **71**: 525–8. doi: [https://doi.org/10.1016/0030-4220\(91\)90354-F](https://doi.org/10.1016/0030-4220(91)90354-F)
9. Hudgins PA, Gussack GS. MR imaging in the management of extracranial malignant tumors of the head and neck. *AJR Am J Roentgenol* 1992; **159**: 161–9. doi: <https://doi.org/10.2214/ajr.159.1.1609691>
10. Hole KH, Axcrona K, Lie AK, Vlatkovic L, Geier OM, Brennhovd B, et al. Routine pelvic MRI using phased-array coil for detection of extraprostatic tumour extension: accuracy and clinical significance. *Eur Radiol* 2013; **23**: 1158–66. doi: <https://doi.org/10.1007/s00330-012-2669-x>
11. Orhan K, Nishiyama H, Tadashi S, Murakami S, Furukawa S. Comparison of altered signal intensity, position, and morphology of the TMJ disc in MR images corrected for variations in surface coil sensitivity. *Oral Surg Oral Med Oral Pathol Oral Radiol Endod* 2006; **101**: 515–22. doi: <https://doi.org/10.1016/j.tripleo.2005.04.004>
12. Hayes CE, Hattes N, Roemer PB. Volume imaging with MR phased arrays. *Magn Reson Med* 1991; **18**: 309–19. doi: <https://doi.org/10.1002/mrm.1910180206>
13. Way L. *Phased array coil. MR field notes. vol. 1*. Little Chalfont, UK: GE Healthcare; 2005. pp. 1–12.
14. Vovk U, Pernuš F, Likar B. A review of methods for correction of intensity inhomogeneity in MRI. *IEEE Trans Med Imaging* 2007; **26**: 405–21. doi: <https://doi.org/10.1109/TMI.2006.891486>
15. Lin FH, Chen YJ, Belliveau JW, Wald LL. Removing signal intensity inhomogeneity from surface coil MRI using discrete wavelet transform and wavelet packet. *IEEE* 2001; **2001**: 96–111.
16. Murakami S, Verdonschot RG, Kataoka M, Kakimoto N, Shimamoto H, Kreiborg S. A standardized evaluation of artefacts from metallic compounds during fast MR imaging. *Dentomaxillofac Radiol* 2016; **45**: 20160094. doi: <https://doi.org/10.1259/dmfr.20160094>
17. ASTM F2119-07. *Standard test method for evaluation of MR image artifacts from passive implants*. West Conshohocken, PA: ASTM International; 2013.
18. National Electrical Manufacturers Association. *NEMA Standards Publication MS. Determination of image uniformity in diagnostic magnetic resonance images*. Rosslyn, Virginia: National Electrical Manufacturers Association; 2008.
19. American College of Radiology (ACR). *Phantom test guidance for the ACR MRI accreditation program*. Reston, VA: ACR; 1998.
20. Gupta SN, Gupta VS, White AC. Spectrum of intracranial incidental findings on pediatric brain magnetic resonance imaging: what clinician should know? *World J Clin Pediatr* 2016; **5**: 262–72. doi: <https://doi.org/10.5409/wjcp.v5.i3.262>
21. Harms SE, Wilk RM, Wolford LM, Chiles DG, Milam SB, Stephen Milam DB. The temporomandibular joint: magnetic resonance imaging using surface coils. *Radiology* 1985; **157**: 133–6. doi: <https://doi.org/10.1148/radiology.157.1.4034958>
22. Amin N, Afzal M. The impact of variation in the pulse sequence parameters on image uniformity in magnetic resonance imaging. *J Pak Med Assoc* 2009; **59**: 231–5.
23. Ogasawara G, Inoue Y, Matsunaga K, Fujii K, Hata H, Takato Y. Image non-uniformity correction for 3-T Gd-EOB-DTPA-enhanced MR imaging of the Liver. *Magn Reson Med Sci* 2017; **16**: 115–22. doi: <https://doi.org/10.2463/mrms.mp.2016-0012>
24. Zhou Y. SU-E-I-35: Investigation of commercially available image uniformity filters in MRI Imaging. *Med Phys* 2014; **41**: 137–8. doi: <https://doi.org/10.1118/1.4887983>
25. Roach M. Base metal alloys used for dental restorations and implants. *Dent Clin North Am* 2007; **51**: 603–27. doi: <https://doi.org/10.1016/j.cden.2007.04.001>
26. Saini M, Singh Y, Arora P, Arora V, Jain K. Implant biomaterials: a comprehensive review. *World J Clin Cases* 2015; **3**: 52. doi: <https://doi.org/10.12998/wjcc.v3.i1.52>
27. Destine D, Mizutani H, Igarashi Y. Metallic artifacts in MRI caused by dental alloys and magnetic keeper. *J Jpn Prosthodont Soc* 2008; **52**: 205–10. doi: <https://doi.org/10.2186/jjps.52.205>